Catal Lett (2015) 145:1837–1844
DOI 10.1007/s10562-015-1593-5

One-Pot Synthesis of Monodisperse Palladium Tin Nanoparticles with Controlled Composition and Size and Its Catalytic Ability Study

Yong Li[1] · Yu Dai[1] · Xi-ke Tian[1]

Received: 3 May 2015 / Accepted: 15 July 2015 / Published online: 4 August 2015

Abstract We have developed a novel one-pot synthetic procedure for monodisperse palladium tin bimetallic alloy nanoparticles (NPs) with tunable compositions and sizes by the co-reduction of tin(II) acetate and palladium(II) bromide in the presence of oleylamine and trioctylphosphine. These NPs loaded on active carbon (PdSn/C) were used as active catalysts for Heck reactions, and exhibited composition dependent catalytic activities. Among these nanocatalysts, $Pd_{63}Sn_{37}$ NPs showed the best catalytic performance which is even superior to pure Pd NPs.

Graphical Abstract PdSn NPs with controlled compositions and sizes were synthesized and characterized systematically, and $Pd_{63}Sn_{37}$/C NPs showed the best catalytic ability and stability that is even superior to pure Pd NPs with higher catalytic activity and stability in multi-recycled Heck reactions.

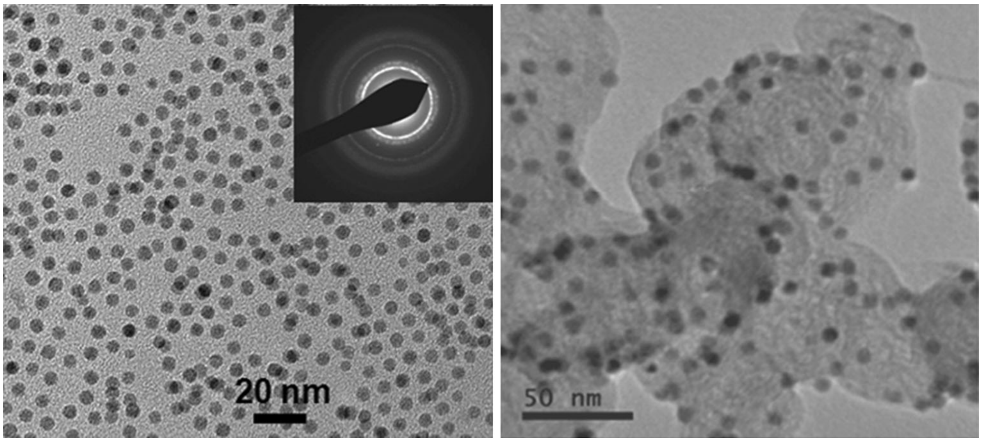

Keywords Palladium tin nanoparticles · Controlled composition and size · Transmission electron microscope · Heck reaction

1 Introduction

The olefination of aryl halides (Heck reaction) is one of the most important reactions used to generate new carbon–carbon bond [1]. This reaction is often catalyzed by

---

Electronic supplementary material The online version of this article (doi:10.1007/s10562-015-1593-5) contains supplementary material, which is available to authorized users.

✉ Xi-ke Tian
xktian@cug.edu.cn

[1] Faculty of Material Science and Chemistry, China University of Geosciences, Wuhan 430074, People's Republic of China

palladium (Pd) complex of phosphines, amines or heterocyclic carbenes in homogeneous solutions under inert atmosphere with good synthetic yields [2]. However, these Pd-complex catalysts do have their limitations. They are only active when the Pd(II) is reduced to Pd(0), which requires the reaction to proceed under a non-oxidizing environment; the active Pd(0) intermediate species are unstable in the reaction conditions and tend to aggregate into inactive components, making it impossible to recycle them for further use; the Pd(II) and Pd(0) as well as the specially chosen ligands contaminate the reaction product and must be removed from the product via tedious separation process before the newly prepared organic compounds can be used for further applications [3]. To overcome these problems associated with the previous catalysts, novel catalyst systems are also developed and tested.

These novel catalysts are either Pd complexes or Pd-based elemental, alloy and core/shell nanoparticles (NPs) supported on various forms of carbons, oxides, polymer resins, or even magnetic NPs [4–9]. Mahmoud Nasrollahzadeh has prepared Pd/CuO NPs for Heck coupling reactions with the high yields, simple methodology, easy preparation and handling of the catalyst and also easy work up [10]. Pd NPs also can be supported on pectin and gelatin, respectively to exhibit a high activity toward Heck reaction, and the catalysts can be recycled for several runs without any losses of catalytic ability [11, 12]. Pd NPs on amino-vinyl silica functionalized Fe_3O_4 magnetic NPs were also applied as nanocatalysts for Heck reaction and the catalysts were recoverable magnetically and could be reused for five runs without significant loss of catalytic activity [13]. Among a great number of Pd based NPs for Heck reaction, bimetallic Pd alloy NPs are particularly important in the area of catalysis because they often exhibited high catalytic ability than their monometallic counterparts [14]. For Pd alloy NPs, mixing a second non-precious element with Pd metal is an effective way to reduce the precious metal usage and may enhance its internal properties due to synergistic effects and the rich diversity of the compositions [15, 16]. Seong-Ho Choi synthesized a series of Pd alloy NPs, such as PdAg, PdNi, and PdCu NPs for Heck reactions, and found the NPs showed excellent capabilities as catalysts for Heck reactions with the comparable catalytic ability of Pd NPs [17]. Palladium tin (PdSn) alloy nanostructures have attracted intense attention in both synthesis and catalysis fields. Earlier studies have shown that PdSn is an active catalyst for hydrogenation of chloro(Cl)-benzene as Sn on PdSn has higher affinity for the chloride, stabilizing Pd against oxidation by Cl [18]. PdSn alloys are also active for hydrogenolysis reactions and their activity are Pd/Sn composition dependent [19]. The reason for high catalytic ability of PdSn NPs is mainly due to the unique characteristics of tin. And the unique characteristics of tin are probably attributed to the strong metal-support interaction and/or the alloy formation between tin and precious metal, such as Pd and Pt [20]. In other words, some electronic effects are of interesting importance for the enhanced performance of tin. For instance, in electronic effects, tin could modify the electronic density of Pt due to positive charge transfer from Snn + species to noble metals, such as Pd and Pt, and the formation of different alloys of Pd-Sn and Pt–Sn. These modifications may be responsible for some changes in the heat of adsorption of different adsorbates, facilitating the reaction [21, 22]. Previous studies also indicated that the compositions or morphologies of PdSn alloy NPs can be controlled by tuning the amount of the precursors. In the literature, PdSn NPs were synthesized by traditional co-reduction of Pd and Sn salts directly on various supporting materials such as amorphous carbon [23]. However, all the reported syntheses did not provide sufficient control over the morphology and composition of the NPs simultaneously to meet the high standard of a catalyst [24].

Recently a facile synthetic approach of monodisperse Pd NPs, Pd alloy and PtSn NPs was developed systematically [25, 26]. We found that the synthesis could be extended to PdSn as well and monodisperse PdSn alloy NPs with compositions and sizes controlled. Herein, we report the one-pot preparation of monodisperse PdSn alloy NPs and study their catalytic abilities for Heck reaction between aryl halides and styrene. We studied the catalytic properties of $Pd_{77}Sn_{23}$, $Pd_{67}Sn_{33}$, $Pd_{63}Sn_{37}$, $Pd_{52}Sn_{48}$ and $Pd_{49}Sn_{51}$ for model Heck reaction and found their catalytic abilities are highly composition dependent. They were indeed more active and stable catalyst than pure Pd NPs with $Pd_{63}Sn_{37}$ NPs being the most active one due to its high catalytic ability, low active species leaching and high stability during the recycle Heck reactions. In addition, $Pd_{63}Sn_{37}$ NPs can be extended to be applied in a number of similar Heck reactions, indicating that this kind of nanocatalysts provide a new synthetic approach for carbon coupling reactions.

2 Experimental Section

2.1 Materials and Characterization Techniques

Palladium(II) bromide ($PdBr_2$, 99 %), Tin(II) acetate ($Sn(ac)_2$, 99 %), oleylamine (OAm, technical grade, 70 %), trioctylphosphine (TOP, technical grade, 90 %), acetic acid, tributylamine borane complex (TBAB), Et_3N, Na_2CO_3, $NaHCO_3$, Na_3PO_4, chlorobenzene, bromobenzene, iodobenzene, *N*-methylpyrrolidone (NMP), *N*,*N*-dimethylacetamide (DMAc), *N*-dimethylformide (DMF), and triethylamine (Et_3N) were purchased from Sigma-Aldrich and Strem Chemicals and used without further purification. Carbon black (Ketjen EC 300 J) is purchased from the Ketjen Black International Company, Japan. Water used in the experiments was deionized (DI) and doubly distilled prior to use.

Transmission electron microscopy (TEM) images were acquired on a Philips CM 20 (200 kV) transmission electron microscope. High resolution transmission electron microscopy (HRTEM) images are obtained with JEOL 2010 (200 kV) and JEOL 4000 EX transmission electron microscopes. X-ray powder diffraction (XRD) patterns of the samples were recorded on a Bruker AXS D8-Advanced diffractometer with Cu Kα radiation ($\lambda = 1.5418$ Å). The compositions of the samples were measured by Inductively Coupled Plasma–Atomic Emission Spectroscopy (ICP–AES). The Heck reaction products were determined by gas chromatography method.

2.2 Synthesis of PdSn NPs

In a typical synthesis for $Pd_{77}Sn_{23}$ NPs, 0.2 mmol $PdBr_2$ and 0.05 mmol $Sn(ac)_2$ were mixed with 12 ml OAm in the reaction flask with magnetic stirring and degassed at room temperature for 10 min under N_2 flow. 0.5 ml TOP was added into the degassed reaction mixture and the mixture was degassed at room temperature for another 30 min before being quickly heated up to 260 °C with in 10 min; the reaction was maintained at this temperature for 1 h to complete the synthesis. After it was cooled to room temperature, the $Pd_{77}Sn_{23}$ NPs were precipitated out through ethanol addition and collected through centrifugation. The $Pd_{77}Sn_{23}$ NPs were redispersed in hexane and washed twice with hexane and ethanol mixture. Finally the as prepared $Pd_{77}Sn_{23}$ NPs was dispersed and stored in hexane.

Composition control of the PdSn NPs: the composition control was achieved simply by changing the molar ration of $PdBr_2/Sn(ac)_2$ used in the synthesis. For $PdBr_2/Sn(ac)_2$ (mmol/mmol) of 0.2/0.07, 0.2/0.1, 0.2/0.15, 0.2/0.2, PdSn NPs with Pd/Sn atomic ratios of 67/33, 63/37, 52/48, 49/51 were synthesized respectively. Size control of the PdSn NPs: the size control was achieved by controlling the amount of TOP in the synthesis. In the synthesis, 6.5, 8 and 9.5 nm PdSn alloy NPs were synthesized by using 0.5, 0.75, 1.0 mL TOP.

2.3 Preparation of Catalysts: PdSn/C

Ten milligram of PdSn NPs were dispersed in 10 mL hexane in a 20 mL vial and 10 mg of Ketjen carbon support was carefully added to it. This mixture was sonicated for 2 h to load all PdSn NPs on carbon (denoted PdSn/C). PdSn/C was separated from hexane by centrifugation and then dispersed in acetic acid. PdSn/C and acidic acid mixture was heated at 70 °C for 10 h to clean the surfaces of NPs. After cooled to room temperature, PdSn/C were separated by adding 30 mL of ethanol and centrifugation, followed by extra two ethanol washes to clean all acid residues. PdSn/C catalysts were dried, weighed and finally dispersed in a measured amount of de-ionized water by 1 h sonication, resulting in 2 mg PdSn/C nanocatalysts per 1 mL water dispersion.

2.4 General Procedure for the Catalytic Tests

The model Heck reaction of bromobenzene and styrene was performed. Typically, the as-prepared 2 mg nanocatalyst was added into the mixture solution of 10 mmol bromobenzene, 20 mmol base and 5 mL organic solvent. The mixture solution was preheated for 1 h, and then 12 mmol styrene was added, and the solution was refluxed and stirred for 6 h. After that, the catalysts were filtered via hot filtration, and the filtrated solution was collected and evaporated to get a white solid. The product was purified by column chromatography. Pd content in the product solution was analyzed using an ICP–AES. The experiments were repeated with the catalyst recycled from last reaction.

3 Results and Discussion

The monodisperse $Pd_{77}Sn_{23}$ NPs was synthesized by quickly heating up a solution of 0.2 mmol $PdBr_2$, 0.05 mmol $Sn(ac)_2$, 0.5 mL TOP and 12 mL OAm to 260 °C and maintained at this temperature for 1 h. The presence of TOP was important to initiate co-reduction of $PdBr_2$ and $Sn(ac)_2$ for PdSn nucleation and growth. Without TOP, a mixture of Pd and Sn NPs was formed. The composition of the PdSn NPs measured by ICP–AES was controlled by the molar ratio of the metal precursors. When $PdBr_2/Sn(ac)_2$ (mmol/mmol) = 0.2/0.05, 0.2/0.07, 0.2/0.1, 0.2/0.15, 0.2/0.2, PdSn NPs with different molar ratios of $Pd_{77}Sn_{23}$, $Pd_{67}Sn_{33}$, $Pd_{63}Sn_{37}$, $Pd_{52}Sn_{48}$ and $Pd_{49}Sn_{51}$ were obtained respectively, and the atomic ratio of Pd in the precursors was carried over to the final product. Further increase of the $Sn(ac)_2$ to 0.25 mmol cannot lead to further increase of Sn in the NPs, and the excess $Sn(ac)_2$ leads to a polydisperse and ununiform product (Fig. S1f). So this synthesis has a limited control over the composition with the Pd_1Sn_1 to be the Sn rich end. It looks that under current synthetic conditions, Sn-rich PdSn alloy NPs could not be synthesized.

Figure 1 is the representative TEM image of the $Pd_{77}Sn_{23}$ NPs with an average diameter of 6.5 ± 0.5 nm. TEM images of other PdSn NPs are given in Fig. S1(a–e). The sizes of all PdSn NPs prepared here are around 6.5 nm, and

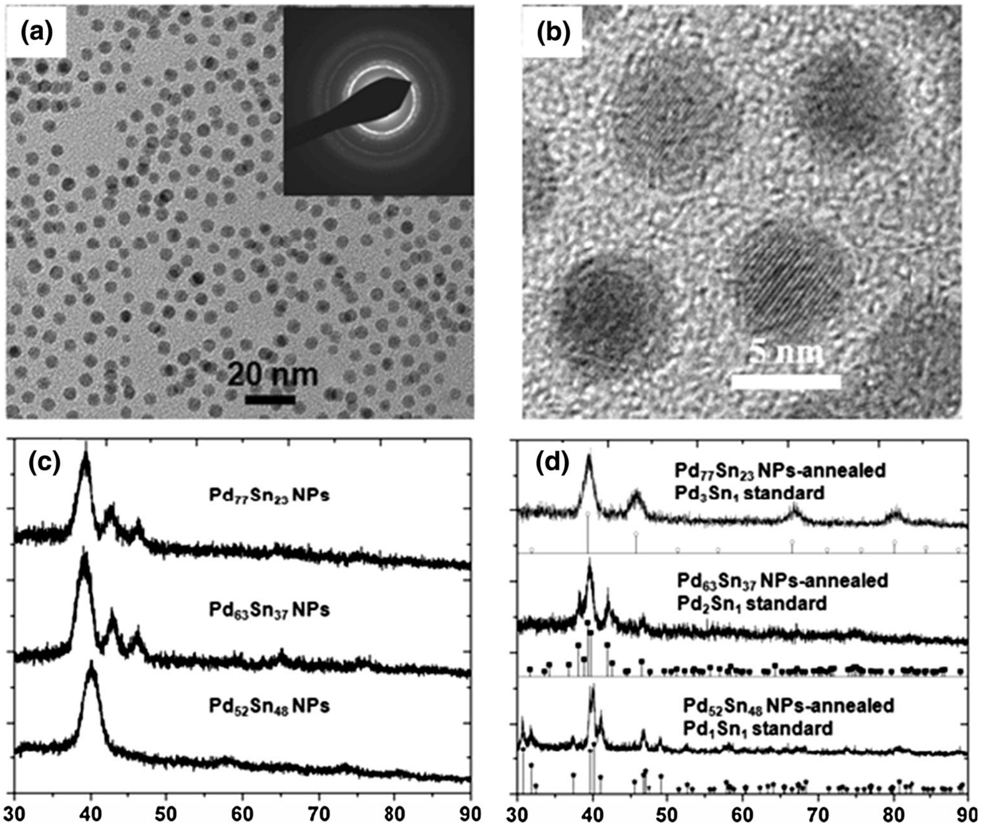

Fig. 1 **a** TEM image and SAED (*inset*), **b** HRTEM image of the as prepared $Pd_{77}Sn_{23}$ NPs, XRD patterns of the as prepared $Pd_{77}Sn_{23}$, $Pd_{63}Sn_{37}$ and $Pd_{52}Sn_{48}$ NPs (**c**) and the crystallized NPs after thermal treatment (**d**)

the detailed sizes of the NPs were listed in Table S1. In addition, while keeping the composition constant, we could tune the sizes of the NPs by varying the amount of TOP added in the reaction. For example, 6.5, 8, and 9.5 nm $Pd_{77}Sn_{23}$ NPs (Fig. S2) were synthesized by using 0.5, 0.75, 1.0 mL TOP. It seems that more TOP can protect Pd via Pd-TOP from the formation of PdSn nuclei in the reaction mixture, allowing more Pd (and Sn) to grow around the existing nuclei into larger NPs. The as-synthesized PdSn NPs are in polycrystalline structure as indicated by diffused diffraction rings observed in the selected area electron diffraction pattern (SAED, Fig. 1a inset). High resolution TEM (HRTEM) image of the single $Pd_{77}Sn_{23}$ NPs (Fig. 1b) show the smaller crystal domains on each NP with crystal lattice fringes at 0.226 nm, corresponding to (111) crystal planes. X-ray diffraction (XRD) was further used to characterize the structure of the as prepared PdSn NPs. Fig. 1c is the XRD patterns of the $Pd_{77}Sn_{23}$, $Pd_{63}Sn_{37}$ and $Pd_{52}Sn_{48}$ NPs. The broad XRD diffraction peaks agree with the polycrystalline nature. However, the XRD peaks of the as prepared PdSn NPs cannot be simply ascribed to any Pd_3Sn_1, Pd_2Sn_1, Pd_1Sn_1 or Pd phases. To identify the crystal phases, we heated the as prepared NPs at elevated temperatures in Argon. The $Pd_{77}Sn_{23}$ NPs after high temperature crystallization showed a cubic Pd_3Sn_1 phase. And the $Pd_{63}Sn_{37}$ NPs and $Pd_{52}Sn_{48}$ NPs after annealing showed orthorhombic Pd_2Sn_1 and Pd_1Sn_1 crystal phases, respectively (Fig. 1d). The XRD characterizations demonstrate that by controlling Pd/Sn composition, we can obtain PdSn NPs with different crystal phases. Our synthesis is advantageous compared to what have been reported. For example, the PdSn NPs made from β-Sn nanocube templates only show Pd_1Sn_1 crystal phase [27]. The PdSn NPs formed directly on carbon support have an fcc structure same as Pd, and the doping of Sn atoms leads to a lattice change [28]. It looks that in these two studies, only a small amount of Sn was successfully alloyed with Pd, as seen from the phase diagram of Pd-Sn system [29], the fcc solid solution with a Pd structure only exists at Pd rich end (at.% of Pd >84.5 %). Our synthesis is carried out at a temperature as high as 260 °C that benefits alloy formation, thus our synthesis leads to the formation PdSn NPs with controlled alloy structure.

To apply the PdSn NPs as nanocatalysts for Heck reactions, the as prepared PdSn NPs (20 mg) were loaded onto carbon black (20 mg) (denoted as PdSn/C) by sonication followed by acetic acid cleaning. The PdSn NPs are well dispersed on the carbon support as shown in the TEM image (Fig. 2). For Heck reaction of bromobenzene and styrene, reaction parameters, such as temperature, organic solvent, and base are quite important. As shown in Table S2, the optimum reaction parameters for Heck

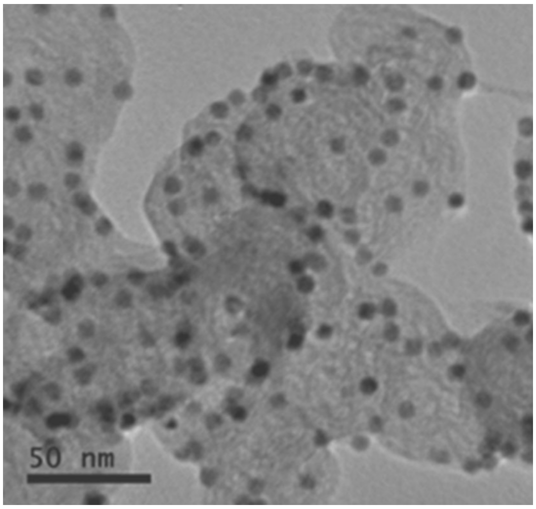

Fig. 2 TEM images of $Pd_{63}Sn_{37}/C$ NPs before catalytic reaction

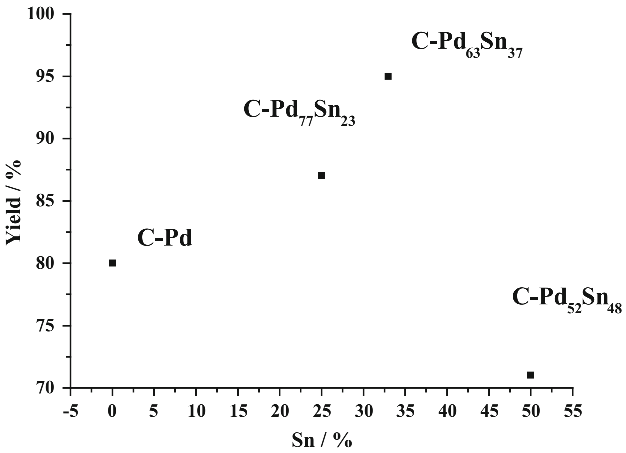

Fig. 3 Corresponding yield—Sn molar percentage curve for Pd/C and PdSn/C NPs

reaction are Et_3N as the base, DMF as solvent and 140 °C as reaction temperature. Under the reaction conditions, we evaluated the influence of PdSn/C alloy composition on catalytic performances. The correlation of Pd/Sn composition versus yield is plotted in Fig. 3. For comparison, Pd/C NPs with the size of 6.3 ± 0.5 nm were prepared according to previous literatures [27]. Pd/C and PdSn/C NPs are active nanocatalysts for Heck reaction with the yields in the range of 71–95 %. For Pd/C, $Pd_{77}Sn_{23}/C$ and $Pd_{63}Sn_{37}/C$ NPs, the yield increased 80, 87–95 % with Sn content increasing. However, further increase of Sn to $Pd_{52}Sn_{48}$ reduced the yield to 71 %. This demonstrates that the addition of appropriate amount of Sn can greatly improve the catalytic performance. The enhancement probably results from the electronic effect of Sn. The addition of Sn in our study would lead to a decrease of Pd (3d) binding energy, change the electronic structure of Pd and density of state of metal catalysts, and weaken the energy of carbon and substituted atoms bond [30, 31], which probably influences the chemisorption energy of intermediates on the catalysts. In addition, the NPs with smaller particle sizes display a higher core-level binding energy shift and a higher valence band centre downshift with respect to the Fermi level. According to the density functional theory of heterogeneous catalysis and mechanistic considerations, the observed valence band centre downshifts can cause a weakening of the bond strength of the reactants adsorbed on the catalyst surface, which results in the increase in the yield of Heck reaction [32]. So although Sn itself has no catalytic activity, it functions as a co-catalyst, and the addition of appropriate amount of Sn a pivotal factor influencing the catalytic performance for Heck reaction.

The stability and reusability of $Pd_{63}Sn_{37}/C$ NPs on Heck reaction were further evaluated. We conducted catalysis reaction with free standing $Pd_{63}Sn_{37}$ NPs and found many of them quickly aggregated with each other during, thus decreasing the catalytic ability (Fig. 4a). While $Pd_{63}Sn_{37}/C$ NPs exhibited negligible morphology changes after one catalysis cycle (Fig. 4b). Then $Pd_{63}Sn_{37}/C$ NPs were separated, recovered and reused at least six times without significant loss of catalytic activity (Fig. 5a). The yield of first recycle was 95 %, which is almost the same after six cycles, and $Pd_{63}Sn_{37}/C$ NPs after six cycles were characterized by TEM studies (Fig. 4c). We can see that $Pd_{63}Sn_{37}$ NPs were still well-dispersed on the surface of amorphous carbon and no great changes happened on their morphologies. While the yields of Heck reaction catalyzed by PdAg, PdNi, and PdCu NPs are all about 90 % and the catalytic ability would decrease with the cycles increasing [17], illustrating that $Pd_{63}Sn_{37}$ NPs are effective nanocatalysts for Heck reactions than the previously reported NPs.

Metal leaching is a serious problem for metal catalysts, which prohibits their reaction ability, recycling ability and effectiveness. We monitored Pd leaching of $Pd_{63}Sn_{37}/C$ NPs during the recycle experiments by analyzing the Pd concentration in the extraction solution by ICP–AES analysis. The Pd leaching percentage of $Pd_{63}Sn_{37}/C$ NPs is corresponding to 0.003 % leaching of the original Pd content for the first cycle. After the sixth catalytic cycle, the total Pd leaching is about 0.004 %, indicating that there is no great increase during the recycle reactions (Fig. 5b). While Pd/C NPs showed the Pd leaching of about 1.2 % in the Heck reactions [33]. Pd-silica catalyst-4 reveals that the leaching of Pd into the solution is about 0.2 ppm [34]. Through the comparations with other nanocatalysts, we found $Pd_{63}Sn_{37}/C$ NPs are good catalysts for Heck reaction with little Pd leaching.

We have also conducted the catalyst poisoning experiments to investigate the resistance of $Pd_{63}Sn_{37}/C$ NPs to

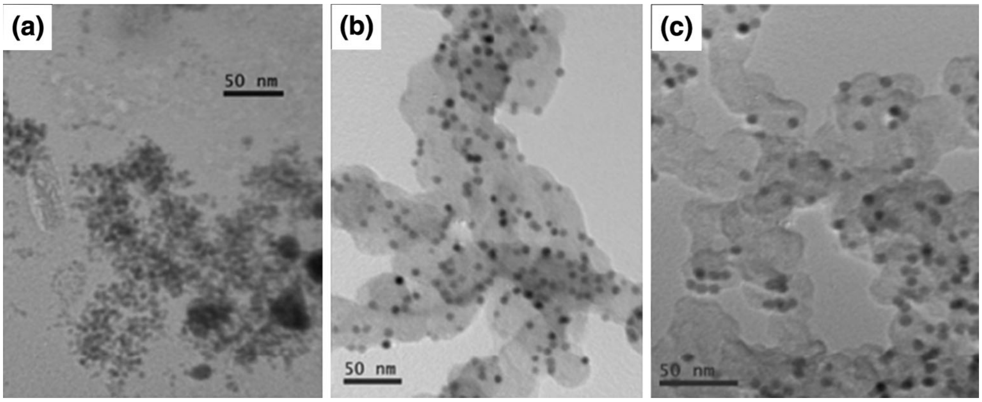

Fig. 4 TEM images of unsupported $Pd_{63}Sn_{37}$ NPs after Heck reaction (**a**), $Pd_{63}Sn_{37}/C$ NPs after one cycle (**b**) and $Pd_{63}Sn_{37}/C$ NPs after six cycles (**c**)

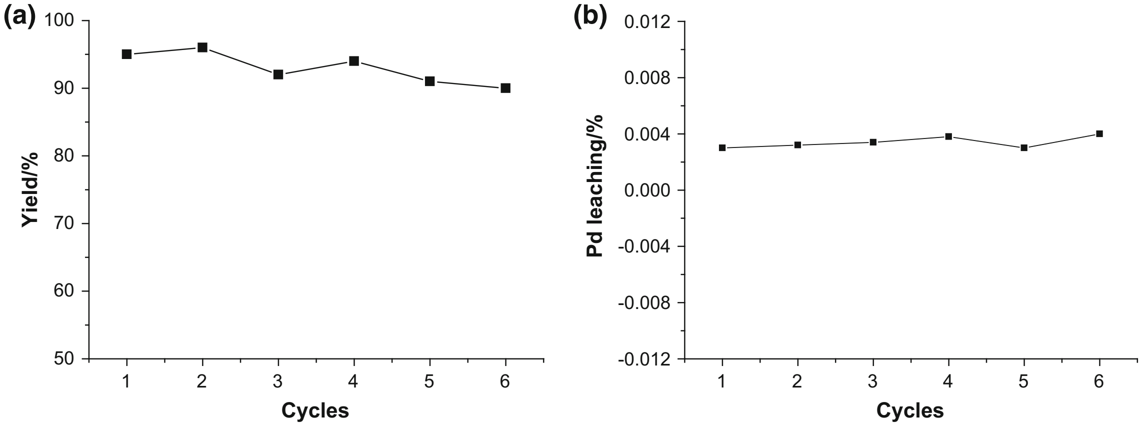

Fig. 5 Yield (**a**) and Pd leaching (**b**) for $Pd_{63}Sn_{37}/C$ NPs in Heck reaction of bromobenzene with styrene

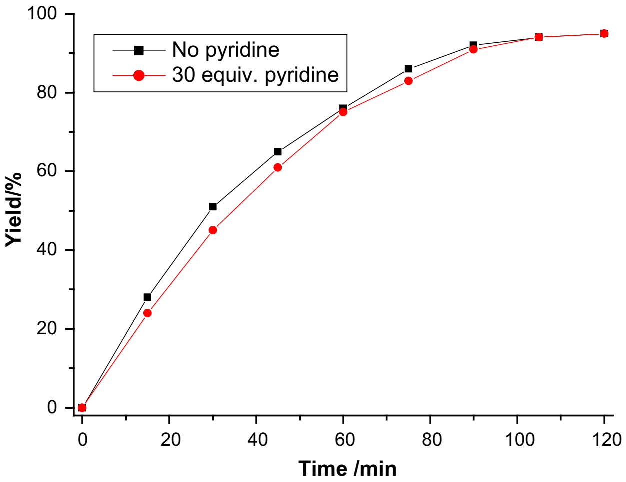

Fig. 6 Plot of yield of Heck reaction of bromobenzene and styrene catalyzed by $Pd_{63}Sn_{37}/C$ NPs versus time with and without pyridine as catalyst poison

poison and aging. Pyridines are known to bind strongly to Pd(II), so pyridines were used as catalyst poison to study the poison and aging resistance. The details of catalyst poisoning experiment were as below. 30 equivalents of pyridine sites were as catalyst poison and added into the mixture solution of bromobenzene and styrene. During the reaction, reaction yields were monitored for every 30 min. For control, the Heck reaction of bromobenzene and styrene were also conducted without catalyst poison, and also the reaction yields were also monitored for every 30 min. As shown from Fig. 6, we noticed that the reaction yields didn't decrease greatly with the addition of catalyst poison pyridine. 30 equivalents of pyridine had almost no poisoning effect on the Heck reaction of bromobenzene and styrene, indicating that the $Pd_{63}Sn_{37}$ NPs possess good resistance against the catalyst poison and aging, and the results are similar to the previously reported Pd-SH-SBA-15 nanocatalyst [35]. In summary, $Pd_{63}Sn_{37}/C$ NPs are

Table 1 Different Heck reactions catalyzed by $Pd_{63}Sn_{37}$/C NPs under optimized conditions

Entry	Ar-X	Alkene	Product	Yield/%[a]
1	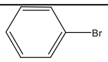	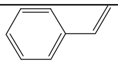	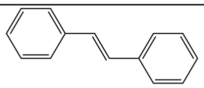	95
2	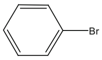	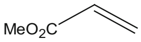	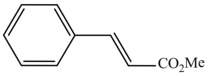	85
3	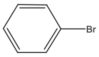	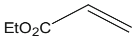	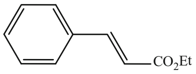	78
4	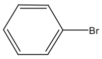	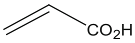	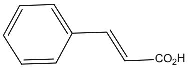	86
5	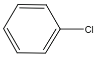	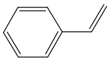	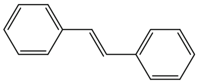	65
6	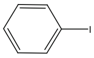	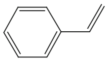	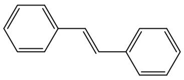	98
7	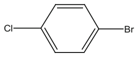	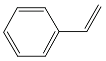	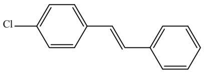	82
8	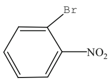	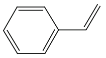	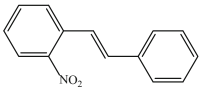	43

Reactions were carried out on a 10 mmol scale in 5.0 mL of organic solvent in air for the specified period of 6 h with 1.0 equiv. of Ar–X, 1.2 equiv. of styrene, 2.0 equiv. of base, and $Pd_{63}Sn_{37}$/C NPs as nanocatalysts

[a] Isolated yields

good nanocatalysts for Heck reaction of bromobenzene and styrene under optimum reaction conditions.

To expand the scope of reaction substrates, different aryl bromides and olefins were employed in Heck reaction to investigate the catalytic ability of $Pd_{63}Sn_{37}$/C NPs, as shown in Table 1. Heck reaction of bromobenzene with methyl acrylate, ethyl acrylate, and acrylic acid afforded good yields (Table 1, entries 2, 3, 4). Heck reactions of styrene and chlorobenzene and iodobenzene were also performed, showing the product yields are different. That is because the electron withdrawing groups facilitate the process of oxidative addition presumably by lowing the energy of the σ* orbital of benzene–halide bonds (Table 1, entries 5, 6) [36]. Chemoselectivity was observed when 1-chloro-4-bromobenzene was employed as the reaction substrate. The reaction was occurred exclusively with aryl bromides, but not aryl chlorides, and gave corresponding product with excellent yield (Table 1, entry 7). Moderate yield of the product was obtained from the coupling reaction between 1-bromo-2-nitrobenzene and styrene (Table 1, entry 8). These experimental results indicated that this reaction was highly sensitive to both steric hindrance and electron efforts because methyl and nitro have similar size but methyl is a mild electron-donating group while nitro is a strong electron-withdrawing one.

4 Conclusions

In summary, we have reported a unique solution phase synthesis of monodisperse PdSn NPs with the controlled sizes and compositions, and then their catalytic activities for Heck reactions were investigated systematically. The PdSn NPs showed the composition dependent catalytic ability with $Pd_{63}Sn_{37}$ being the most active one. The Heck reaction yield catalyzed by $Pd_{63}Sn_{37}/C$ NPs is as high as 95 %, and the reaction yield is almost the same with the cycle experiments. All these show that $Pd_{63}Sn_{37}/C$ NPs are the efficient nanocatalysts for Heck reactions with low leaching, high stability and reusability, and they are of great importance for practical applications.

Acknowledgments This work is supported by Fundamental Research Funds for the Central Universities (CUG120802).

References

1. Corbet JP, Mignani G (2006) Chem Rev 106:2651
2. Littke AF, Fu GC (2005) Org Synth 81:63
3. Astruc D, Lu F, Aranzaes JR (2005) Angew Chem Int Ed 44:7852
4. Jiang HL, Xu Q (2011) J Mater Chem 21:13705
5. Das DD, Sayari AJ (2007) Catal 246:60
6. Shin JY, Lee BS, Jung Y, Kim SJ, Lee SG (2007) Chem Commun 48:5238
7. Choudary BM, Madhi S, Chowdari NS, Kantam ML, Sreedhar B (2002) J Am Chem Soc 124:14127
8. Chen X, Hou Y, Wang H, Cao Y, He J (2008) J Phys Chem C 112:8172
9. Gopidas KR, Whitesell JK, Fox MA (2003) Nano Lett 3:1757
10. Nasrollahzadeh M, Sajadi SM, Rostami-Vartooni A, Bagherzadeh M (2015) J Colloid Interf Sci 448:106
11. Khazaei A, Rahmati S, Hekmatian Z, Saeednia S (2013) J Mol Catal A 372:160
12. Firouzabadi H, Iranpoor N, Ghaderi A (2011) J Mol Catal A 347:38
13. Banazadeh A, Pirisedigh A, Aryanasab F, Salimi H, Shafiei-Haghighi S (2015) Inorg Chim Acta 429:132
14. Sun D, Mazumder V, Metin Ö, Sun S (2012) ACS Catal 2:1290
15. Edwards JK, Hutchings GJ (2008) Angew Chem Int Ed 47:9192
16. Bao J, Chen W, Liu TT, Zhu YL, Jin PY, Wang LY, Liu JF, Wei YG, Li YD (2007) ACS Nano 1:293
17. Kim SJ, Oh SD, Lee S, Choi SH (2008) J Ind Eng Chem 14:449
18. Coq B, Ferrat G, Figueras F (1986) J Catal 101:434
19. Chou NH, Schaak RE (2007) J Am Chem Soc 129:7339
20. Lorenz H, Zhao Q, Turner S, Lebedev OI, Tendeloo VG, Klotzer B, Rameshan C, Pfaller K, Konzett J, Penner S (2010) Appl Catal A 381:242
21. Pisduangdaw S, Panpranot J, Methastidsook Ch, Chaisuk Ch, Faungnawakij K, Praserthdam P, Mekasuwandumrong O (2009) Appl Catal A 370:16
22. Esmaeili E, Rashidi AM, Khodadadi AA, Mortazavi Y, Rashidzadeh M (2014) Fuel Process Technol 120:113
23. Liu Z, Zhang X (2009) Electrochem Commun 11:1667
24. Menzel M, Mehner H, Mönnich I, Berndt H (2000) Hyperfine Interact 126:89
25. Li Y, Dai Y, Yang ZY, Li TR (2014) Inorg Chim Acta 414:59
26. Liu Y, Li D, Stamenkovic VR, Soled S, Henao JD, Sun S (2011) ACS Catal 1:1719
27. Ramulifho T, Ozoemen KI, Modibedi RM, Jafta CJ, Mathe MK (2013) J Electroanal Chem 692:26
28. Zhang Z, Ge J, Ma L, Liao J, Lu T, Xing W (2009) Fuel Cells 2:114
29. Massalski TB (1990) Binary alloy phase diagrams, vol 3, 2nd edn. ASM, Metal Park, p 3049
30. Frelink T, Visscher W, van Veen JAR (1995) Surf Sci 335:353
31. Park KW, Choi JH, Kwon BK, Lee SA, Sung YE, Ha HY, Hong SA, Kim H, Wieckowski A (2002) J Phys Chem B 106:1869
32. Zhou WP, Lewera A, Larsen R, Masel RI, Bagus PS, Wieckowski A (2006) J Phys Chem B 110:13393
33. Heidenreich RG, Krauter Jürgen GE, Pietsch J, Köhler K (2002) J Mol Catal A 182–183:499
34. Polshettiwar V, Molnar A (2007) Tetrahedron 63:6949
35. Richardson JM, Jones CW (2007) J Catal 251:80
36. Cheng M, Yan J, Hu F, Chen H, Hu Y (2013) Chem Sci 4:526